Available online at www.sciencedirect.com
ScienceDirect
Surface Science 601 (2007) L109–L113
SURFACE SCIENCE
www.elsevier.com/locate/susc

Surface Science Letters

Surface plasmon excitation at a Au surface by 150–40,000 eV electrons

Wolfgang S.M. Werner [a,*], Michael R. Went [b], Maarten Vos [b]

[a] *Institut für Allgemeine Physik, Vienna University of Technology, Wiedner Hauptstraße 8–10, A 1040 Vienna, Austria*
[b] *Atomic and Molecular Physics Laboratories, Research School of Physical Sciences and Engineering, Australian National University, Canberra, ACT 0200, Australia*

Received 12 June 2007; accepted for publication 29 June 2007
Available online 13 July 2007

Abstract

Spectra of electrons with energies between 5 and 40 keV reflected from a homogeneous Au surface have been measured and analyzed to give the normalized distribution of energy losses in a single surface and volume excitation, as well as the total probability for excitation of surface plasmons. The resulting single scattering loss distributions compare excellently in (absolute units) with data from previous work taken at lower energies (150–3400 eV). An empirical relationship is derived for the total surface excitation probability as a function of the energy. For high energies the surface scattering zone represents only a small fraction of a typical electron trajectory and hence interference effects should be small at these energies. Since we find that both the energy dependence of the surface plasmon excitation probability and the shape of the single scattering loss distributions are the same at high and low electron energies, we conclude that there is no evidence for interference effects in the entire energy range studied.

Keywords: Au; Electron; Scattering; Inelastic; Elastic; Surface plasmon

While electron energy loss spectroscopy (EELS) in the transmission electron microscope is routinely used to determine the dielectric function of solids for over 30 years [1], extraction of the dielectric function from reflection electron energy loss spectra (REELS) has met with certain difficulties connected with the elimination of multiple scattering effects from experimental spectra. In particular the fact that both surface as well as volume excitations need to be considered for REELS complicates data analysis. Two different approaches to extract the single scattering loss distribution and the optical constants from REELS are presently being investigated: (1) the deconvolution procedure proposed by Tougaard and Chorkendorff [2], in combination with the semiclassical dielectric response model by Yubero and Tougaard [3] (refered to as TCY hereafter); and (2) Ritchie's original model for the single scattering loss distribution in a surface excitation [4–10] applied to deconvoluted spectra obtained by a bivariate reversion of *two* REELS spectra [11–14]. Both approaches are fundamentally different in that TCY assume that it is strictly impossible to separate the contributions of surface and volume excitations in a REELS spectrum due to interference effects between the in- and out-going part of the electron's trajectory [3,15,16]. In the approach based on bivariate reversion of two spectra, separation of the surface and volume components of a REELS spectrum represents the first step. Surface and volume components decomposed in this way have been found to agree well with single scattering loss distributions derived within Ritchie's theory for measurements in the energy range between 150 and 3400 eV [11,12].

In the present paper, high energy REELS data (in the range between 5 and 40 keV) are analyzed and the results are compared with the earlier analysis at lower energies. This is expected to give a clearer insight on the importance of interference effects since the relationship of the mean travelled pathlength and the width of the surface scattering

* Corresponding author. Tel.: +43 1 58801 13462; fax: +43 1 58801 13499.
E-mail address: werner@iap.tuwien.ac.at (W.S.M. Werner).

0039-6028/$ - see front matter © 2007 Elsevier B.V. All rights reserved.
doi:10.1016/j.susc.2007.06.076

zone is quite different at such high energies. The width of the surface scattering zone is given in atomic units as $\langle z_{ss}\rangle = \sqrt{2E}/\omega_s$, where E is the electron energy and ω_s is the surface plasmon frequency [4]. The quantity $\langle z_{ss}\rangle$ varies between $\sim$1 Å at 100 eV and $\sim$10 Å at 40 keV. On the other hand, Monte–Carlo (MC) simulations for the distribution of pathlengths in a REELS experiment show that the mean travelled pathlength $\langle s\rangle$ varies between $\sim$10 Å at 100 eV and $\gtrsim$2000 Å at 40 keV. This implies that for the present data set, the ratio $\langle z_{ss}\rangle/\langle s\rangle$ covers quite a large range between 0.1 and 0.005.

The high energy (5, 10, 20 and 40 keV) REELS spectra analyzed in the present work were obtained on a polycrystalline Au sample using the high-energy electron scattering spectrometer at the Australian National University at a base pressure of 1×10^{-10} mbar [17]. Sample cleaning was performed by Xe^+ ion bombardment and sample cleanliness was monitored by recording low energy REELS spectra (at 1 keV) and comparing these with literature data. The incidence angle was 45°, the emission angle amounted to 45° (all angles with respect to the surface normal), the scattering angle was 120°, the analyzer (half polar) opening angle amounts to about 0.5°. The energy resolution varied with energy but was always better than 0.5 eV (FWHM of the elastic peak). The low energy (150–3400 eV) spectra were taken in a Thermo-VG Microlab 310-F at a base pressure of 1×10^{-10} mbar on a polycrystalline Au film sputter deposited onto a Si wafer. Experimental details are given in Ref. [18]. Here we merely note that the incoming electrons hit the sample along the surface normal, while the analyzer (with a half polar opening angle of about 12°) observes the sample under an angle of 60°. The energy resolution (FWHM) for the low energy data was about 1.5 eV.

Fig. 1 compares the high energy spectra with a pair of spectra taken at lower energies (1000 and 3400 eV). The data are represented by the open circles and have been normalized with the intensity of the elastic peak. Successive spectra are shifted by 0.005 eV^{-1} for clarity. The energy

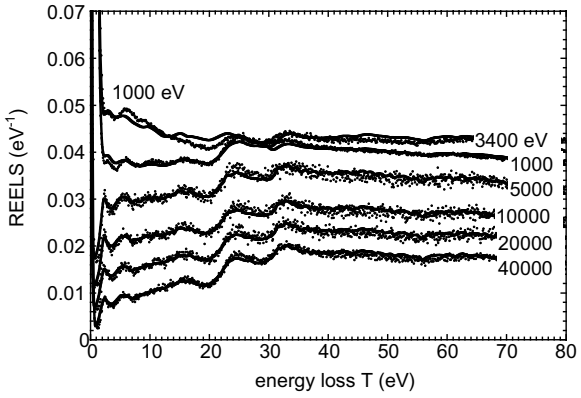

Fig. 1. Experimental REELS spectra (dots) for several energies along with the best fit to Eq. (1) (solid curves) using the average number of surface excitations $\langle n_s\rangle$ as free parameter and the DIIMFP and DSEP retrieved from the high energy data shown in Fig. 3. Successive curves have been shifted by 0.005 units for clarity.

resolution of the low energy data is seen to be slightly worse as for the high energy data, as judged by the width of the elastic peak. The major differences in these spectra are observed at energy losses below $\lesssim$25 eV, being the region where the main influence of surface plasmon excitation is expected (see also Fig. 3 below). It is clearly seen that the surface excitation probability decreases with increasing energy. For energy losses $\gtrsim$25 eV, the spectra are very similar in shape, except for 1000 eV where the intensity decreases faster with increasing energy loss than for the other spectra.

The features seen in the experimental spectra can be quantitatively described by a simple theory by realizing that the recorded intensity consists of groups of electrons that have experienced a certain number (n_b) of volume (or bulk) excitations and (n_s) surface excitations. The relative number of electrons within each group is given by the reduced partial intensity α_{n_b,n_s}. The energy loss distribution of each group is given by $w_s^{(n_s)}(T')\otimes w_b^{(n_b)}(T-T')$ [11], where $w_s^{(n_s)}(T)$ and $w_b^{(n_b)}(T)$ represent the (n_s-1)-fold and (n_b-1)-fold selfconvolution of the normalized single scattering loss distributions. Here $w_s(T)$ is the differential surface excitation probability (DSEP) and $w_b(T)$ denotes the differential inverse inelastic mean free path (DIIMFP), and the symbol $\otimes$ represents a convolution. The spectrum $y(T)$ is a superposition of all groups [11]:

$$y(T)=\sum_{n_b=0}^{\infty}\sum_{n_s=0}^{\infty}\alpha_{n_b,n_s}w_s^{(n_s)}(T')\otimes w_b^{(n_b)}(T-T'). \tag{1}$$

It turns out that the partial intensities for surface and bulk scattering are uncorrelated to a good approximation $\alpha_{n_b,n_s}=\alpha_{n_b}\times\alpha_{n_s}$ [20]. The bulk partial intensities can be calculated by an MC simulation [21], the surface partial intensities follow from the expression for the average number of surface excitations in a single surface crossing [10]

$$\langle n_s\rangle=\frac{a}{\mu\sqrt{E}}, \tag{2}$$

where $\theta=\arccos\mu$ is the polar direction of surface crossing and a is a material parameter, the so–called surface excitation parameter. Assuming that plural surface scattering is governed by Poisson statistics, the reduced surface partial intensities are found as:

$$\alpha_{n_s}=\frac{\langle n_s\rangle^{n_s}}{n_s!}. \tag{3}$$

The reduced volume partial intensities for the present set of experimental data were calculated with the Monte–Carlo method [21] using the TPP-2M formula for the IMFP [22] and the elastic scattering cross sections from Refs. [23,24]. To speed up the calculations, they were performed for a polar semi–angle of detection of 5°. Since the elastic scattering cross section is a smooth function of the scattering angle, this is not expected to lead to any noticeable changes in the *reduced* partial intensities. Representative results are shown in Fig. 2. It is seen that the sequence of

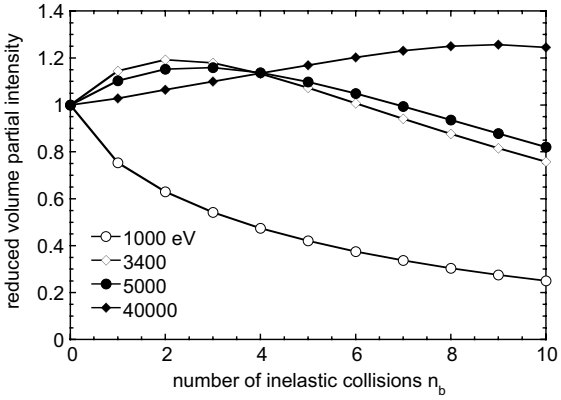

Fig. 2. Volume partial intensities for quasi–elastic electron reflection for the present high energy measurements (filled symbols, 5 and 40 keV, $\arccos\mu_i = 45°$, $\arccos\mu_0 = 45°$) and the data reported in Refs. [19,11] (open symbols, 1000 and 3400 eV, $\arccos\mu_i = 0°$, $\arccos\mu_0 = 60°$).

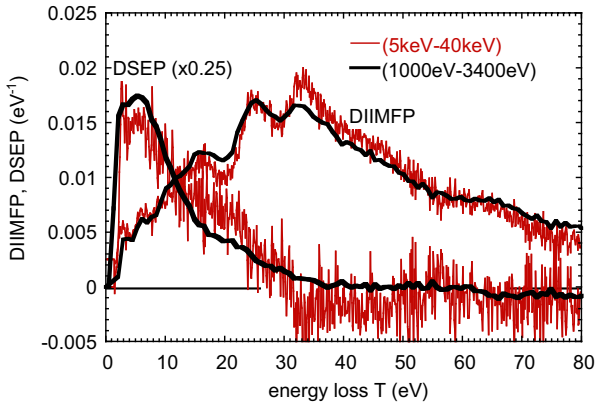

Fig. 3. Comparison of the (normalized) DSEP and DIIMFP retrieved with Eq. (4) from the high energy REELS spectra (5 and 40 keV, $\arccos\mu_i = 45°$, $\arccos\mu_0 = 45°$, thin solid curves) with the results obtained earlier [11] (1000 and 3400 eV, $\arccos\mu_i = 0°$, $\arccos\mu_0 = 60°$, thick solid curves). The data for the DSEP have been scaled by a factor of 0.25, for clarity.

bulk partial intensities is qualitatively different for the various energies and geometrical configurations considered here. For the 1000 eV case, the volume partial intensities decrease monotonically with the scattering order n_b, while for all other cases the sequence of partial intensities exhibits a maximum at a given scattering order. This is attributed to differences in the shape and magnitude of the *elastic* scattering cross section that gives rise to qualitative differences in the path length distribution and the partial intensities [25,20]. Considering that the magnitude of the first order partial intensity is mainly responsible for the first ~50 eV of the loss spectrum, the difference between the REELS spectrum taken using 1000 eV for the primary electrons and the other spectra in Fig. 1 above 30 eV energy loss is explained.

The unique solution of Eq. (1) for the unknowns $w_s(T)$ and $w_b(T)$ can be found by analyzing *two* spectra with different sequences of partial intensities α_{n_b,n_s} and β_{n_b,n_s}, using the formula [11,26]:

$$w(T) = \sum_{k=0}^{2}\sum_{l=0}^{2} a_{k,l}Y_{k,l}(T) - \int_{T'=0}^{T}\sum_{k=0}^{2}\sum_{l=0}^{2} b_{k,l}Y_{k,l}(T-T')w(T')\mathrm{d}T', \quad (4)$$

where the quantity $Y_{k,l}(T)$ is the (k,l)-th order cross convolution of the two REELS spectra. The coefficients $a_{k,l}$ and $b_{k,l}$ in Eq. (4) are functions of the partial intensities of the two spectra [26] and are different for the surface and bulk single scattering loss distribution, the formula for retrieval of the DIIMFP and DSEP is identical and given by Eq. (4).

The result of application of this procedure to the (5000–40,000 eV) and (1000–3400 eV) spectrum pairs shown in Fig. 1 is presented in Fig. 3. The resulting single scattering loss distributions for the high and low energy pair are in good agreement within the experimental accuracy. Note that this comparison is in absolute units. The somewhat noisy nature of the DSEP extracted from the high energy data is a consequence of the fact that the determinant $\Delta = \alpha_{1,0}\beta_{0,1} - \alpha_{0,1}\beta_{1,0}$ is quite small for the high energy case ($\Delta_{5000,40{,}000} = 0.09$) indicating that in the retrieval of the high energy DSEP a small difference between large numbers is being evaluated [11]. In other words, since the contribution of surface excitations is quite small for *both* spectra of the high energy pair, the procedure is close to its numerical limit for extraction of the DSEP. For the low energy pair the determinant is closer to unity ($\Delta_{1000,3400} = 0.35$) and the data for the DIIMFP and DSEP exhibit the same noise level.

Using the DIIMFP and DSEP retrieved from the high energy spectral pair together with the partial intensities calculated by means of MC simulations, the experimental data were fitted to Eq. (1), using the average number of surface excitations $\langle n_s\rangle$ as a fitting parameter and employing Eq. (3). The resulting fit is represented by the solid curves in Fig. 1. It is seen that in this way the experimental spectra over a wide energy range and different scattering geometries, giving rise to qualitatively different sequences of partial intensities (see Fig. 2), are quantitatively accounted for. The corresponding values of $\langle n_s\rangle$ are presented in Fig. 4 as a function of the energy. The low energy data consist of two series of measurements conducted a year apart to check the experimental uncertainty.

Chen [28] proposed that the probability of a surface plasmon excitation would be given by $\langle n_s(\mu,E)\rangle = a/\sqrt{E}\mu$ with a value of $a = 3.06\ \mathrm{eV}^{1/2}$ for Au. Fitting our data with this type of dependence we obtain a reasonable fit with $a = (3.09 \pm 0.05)\ \mathrm{eV}^{1/2}$, in good agreement with the value calculated by Chen. Kwei and coworkers [27] concluded that the dependence should be of the form: $\langle n_s(\mu,E)\rangle = a_2/E^b\mu$, with values for Au of $a_2 = 1.7612\ \mathrm{eV}^{1/2}$ and $b = 0.4404$ for an ingoing and $a_2 = 1.4946\ \mathrm{eV}^{1/2}$ and $b = 0.4208$ for an outgoing surface crossing along the surface normal. Fitting our data with this formula we obtain

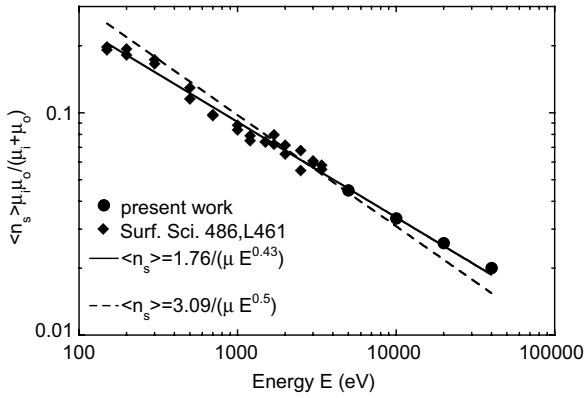

Fig. 4. Surface excitation probability $\langle n_{s,i}+n_{s,0}\rangle\ \mu_i\mu_0/(\mu_i+\mu_0)$ as a function of the energy. Filled circles: present data, filled diamonds: Ref. [19]. The solid and dashed curves are a fit of these data to the functions $\langle n_s(\mu,E)\rangle = a/E^b\mu$ [27] and $\langle n_s(\mu,E)\rangle = a/\sqrt{E}\mu$ [28], respectively.

an excellent fit with $a_2 = (1.76 \pm 0.05)\,\mathrm{eV}^{1/2}$, $b = 0.43 \pm 0.02$, surprisingly close to the values calculated by Kwei and coworkers.

For the high energy data set any eventual interference effect between the in- and out-going part of the trajectory and the concurring interference between surface and bulk excitations predicted by YTC [3,15,16] is expected to be strongly reduced since the surface scattering zone is much smaller than the average pathlength travelled for high energies, $\langle z_{ss}\rangle/\langle s\rangle \sim 0.005$. The surface scattering zone for the high energy data is even much smaller than the pathlength travelled without an inelastic collision, the inelastic mean free path λ (being about 250 Å at 40 keV), implying that $\langle z_{ss}\rangle/\lambda \sim 0.2$. Indeed, the influence of surface excitations for the high energy spectra is much less pronounced at higher energies as seen in Figs. 1 and 4. The retrieved DIIMFP and DSEP nonetheless match the ones at lower energies within the experimental uncertainty. Furthermore, the energy dependence of the total surface excitation probability exhibits the same behaviour for low and high energies, as can be seen from Fig. 4. From these findings it is concluded that interference effects in REELS spectra are too weak to be observed with experiments as the one described in the present paper for the entire energy range investigated, i.e. from 150 to 40 keV. Note that this conclusion is also in perfect agreement with Vicanek's theoretical assessment that such interference effects may be pronounced for individual reflected electrons, but cancel out in a measured REELS due to the broad pathlength distribution giving rise to strong fluctuations in the interference effects that are smeared out accordingly [29].

Recently the magnitude of interference effects as a function of scattering geometry has been studied theoretically [30] for a free electron material (Al), an insulator (SiO_2), a semiconductor (Si) and a transition metal (Cu). The results showed no qualitative differences among these different classes of materials. Significant interference effects were found only for scattering angles in excess of 165°, a situation that is difficult to realize experimentally. Furthermore, a decrease of the magnitude of interference effects with increasing energy was found. The present experiments represent two different scattering geometries that are both typical for REELS and simple to realize experimentally. The experimental energy range includes sufficiently low energies where interference effects should occur. This suggests that interference effects can be generally disregarded when obtaining information on the optical or electronic properties of solids with a typical REELS experiment.

It should finally be noted that the single scattering loss distributions have been used to extract the optical constants of Au from REELS [14] giving good agreement with independent sources of optical data such as density functional theory calculations [31,32] and optical measurements [33] or transmission electron energy loss measurements [34]. On the other hand, Fig. 1 demonstrates that the extracted DIIMFP and DSEP, in combination with realistic partial intensities (see Fig. 2) consistently describe REELS spectra measured over a large energy range and for different scattering geometries, using a *single* fit parameter, the average number of surface excitations in a single surface crossing $\langle n_s\rangle$. The latter quantity also compares well with independent theoretical assessments [28,27], as can be seen from Fig. 4.

Acknowledgements

Financial support of the present work by the Austrian Science Foundation FWF through Project No. P15938-N02 is gratefully acknowledged. Work at the Australian National University was made possible by a grant of the Australian Research Council.

References

[1] R.F. Egerton, Electron Energy Loss Spectroscopy in the Electron Microscope, Plenum, New York and London, 1985.
[2] S. Tougaard, I. Chorkendorff, Phys. Rev. B 35 (1987) 6570.
[3] F. Yubero, S. Tougaard, Phys. Rev. B 46 (1992) 2486.
[4] R.H. Ritchie, Phys. Rev. 106 (1957) 874.
[5] E.A. Stern, R.A. Ferell, Phys. Rev. 120 (1960) 130.
[6] E. Evans, D.L. Mills, Phys. Rev. B 5 (1972) 4126.
[7] E. Evans, D.L. Mills, Phys. Rev. B 7 (1973) 853.
[8] J. Geiger, Phys. Stat. Sol. 24 (1987) 457.
[9] A. Otto, Phys. Stat. Sol. 22 (1967) 401.
[10] C.J. Tung, Y.F. Chen, C.M. Kwei, T.L. Chou, Phys. Rev. B 49 (1994) 16684.
[11] W.S.M. Werner, Phys. Rev. B 74 (2006) 075421.
[12] W.S.M. Werner, Surf. Sci. 588 (2005) 26.
[13] W.S.M. Werner, Surf. Sci. 600 (2006) L250.
[14] W.S.M. Werner, Appl. Phys. Lett. 89 (2006) 213106.
[15] F. Yubero, J.M. Sanz, B. Ramskov, S. Tougaard, Phys. Rev. B 53 (1996) 9719.
[16] A. Cohen-Simonsen, F. Yubero, S. Tougaard, Phys. Rev. B 56 (1997) 1612.
[17] M.R. Went, M. Vos, Appl. Phys. Lett. 90 (2007) 072104.
[18] W.S.M. Werner, C. Tomastik, T. Cabela, G. Richter, H. Störi, J. Electron Spectrosc. Rel. Phen. 113 (2001) 127.
[19] W.S.M. Werner, W. Smekal, C. Tomastik, H. Störi, Surf. Sci. 486 (2001) L461.

[20] W.S.M. Werner, Surf. Interf. Anal. 35 (2003) 347.
[21] W.S.M. Werner, Surf. Interf. Anal. 31 (2001) 141.
[22] S. Tanuma, C.J. Powell, D.R. Penn, Surf. Interf. Anal. 21 (1994) 165.
[23] A. Jabłonski, F. Salvat, C.J. Powell, J. Phys. Chem. Ref. Data 33 (2004) 409.
[24] F. Salvat, R. Mayol, Comp. Phys. Comm. 74 (1993) 358.
[25] W.S.M. Werner, M. Hayek, Surf. Interf. Anal. 22 (1994) 79.
[26] W.S.M. Werner, Surf. Sci. 601 (2007) 2125.
[27] C.M. Kwei, C.Y. Wang, C.J. Tung, Surf. Interf. Anal. 26 (1998) 682.
[28] Y.F. Chen, Surf. Sci. 519 (2002) 115.
[29] M. Vicanek, Surf. Sci. 440 (1999) 1.
[30] N. Pauly, S. Tougaard, F. Yubero, Phys. Rev. B 73 (2006) 035402.
[31] V.J. Keast, J. Electron Spectrosc. Rel. Phen. 143 (2005) 97.
[32] C. Ambrosch-Draxl, J.O. Sofo, Comp. Phys. Comm. 17 (2006) 1.
[33] E.D. Palik, Handbook of Optical Constants of Solids, Academic Press, NewYork, 1985.
[34] J. Daniels, Z. Physik 203 (1967) 235.